Atmospheric Environment 134 (2016) 217–223

Contents lists available at ScienceDirect

Atmospheric Environment

journal homepage: www.elsevier.com/locate/atmosenv

Technical note

An analytical system enabling consistent and long-term measurement of atmospheric dimethyl sulfide

Sehyun Jang [a, 1], Ki-Tae Park [a, b, 1], Kitack Lee [a, *], Young-Sang Suh [c]

[a] School of Environmental Science and Engineering, Pohang University of Science and Technology, Pohang, 790–784, South Korea
[b] Arctic Research Center, Korea Polar Research Institute, Incheon, 406–840, South Korea
[c] National Fisheries Research and Development Institute, Busan, 609–735, South Korea

HIGHLIGHTS

- A fully integrated, automated system for the continuous measurement of airborne DMS.
- The proposed system was proved to be stable for 3 full growth cycles of phytoplankton.
- The system enabled the measurements of short-term and long-term airborne DMS trends.

ARTICLE INFO

Article history:
Received 19 January 2016
Received in revised form
17 March 2016
Accepted 18 March 2016
Available online 22 March 2016

Keywords:
Dimethyl sulfide
Climate feedback
Atmospheric monitoring
Arctic Ocean

ABSTRACT

We describe here an analytical system capable of continuous measurement of atmospheric dimethylsulfide (DMS) at pptv levels. The system uses customized devices for detector calibration and for DMS trapping and desorption that are controlled using a data acquisition system (based on Visual Basic 6.0/C 6.0) designed to maximize the efficiency of DMS analysis in a highly sensitive pulsed flame photometric detector housed in a gas chromatograph. The fully integrated system, which can sample approximately 6 L of air during a 1-hr sampling, was used to measure the atmospheric DMS mixing ratio over the Atlantic sector of the Arctic Ocean over 3 full annual growth cycles of phytoplankton in 2010, 2014, and 2015, with minimal routine maintenance and interruptions. During the field campaigns, the measured atmospheric DMS mixing ratio varied over a considerable range, from <1.5 pptv to maximum levels of 298 pptv in 2010, 82 pptv in 2014, and 429 pptv in 2015. The operational period covering the 3 full annual growth cycles of phytoplankton showed that the system is suitable for uninterrupted measurement of atmospheric DMS mixing ratios in extreme environments. Moreover, the findings obtained using the system showed it to be useful in identifying ocean DMS source regions and changes in source strength.

© 2016 Elsevier Ltd. All rights reserved.

1. Introduction

Dimethyl sulfide (DMS) is a volatile byproduct of the enzymatic breakdown of dimethyl sulfoniopropionate (DMSP), a compound produced by phytoplankton. DMS is a major natural source of tropospheric sulfur, which may have an impact on the radiative balance of the atmosphere (Bates et al., 1987; Simó, 2001). The potential role of marine DMS in regulating climate was highlighted by Charlson et al. (1987). In the proposed mechanism, atmospheric DMS is rapidly oxidized by hydroxyl radicals and is then transformed into sulfuric and methane sulfonic acids, both of which contribute to the formation of cloud condensation nuclei (CCN) (Shaw, 1983; Andreae and Crutzen, 1997). CCN may alter the radiation budget of the atmosphere via albedo change (Andreae and Rosenfeld, 2008), which could consequently influence the amount of incoming solar radiation, and thereby affect the temperature of the upper ocean. Change in the upper ocean temperature may change DMS production by shifting the major phytoplankton species (Simó, 2001; Stefels et al., 2007). Change in the production of DMS could lead to change in the production of CCN (Andreae and Crutzen, 1997). As a result, the production of DMS and regional/global climate may be closely linked. This linkage has yet to be experimentally demonstrated, but such a negative

* Corresponding author.
E-mail address: ktl@postech.ac.kr (K. Lee).
[1] These authors (Sehyun Jang and Ki-Tae Park) contributed equally.

http://dx.doi.org/10.1016/j.atmosenv.2016.03.041
1352-2310/© 2016 Elsevier Ltd. All rights reserved.

feedback mechanism may in part offset the global warming resulting from anthropogenic CO_2 (Charlson et al., 1987).

It is not possible to test whether the production of DMS is positively linked to the production of CCN, because atmospheric DMS measurements lack adequate spatial and temporal coverage. This is largely because the measurement systems used to date have not been sufficiently sensitive, complex, and durable to enable consistent measurement of such short-lived DMS to be made over long periods (seasons to years). Various methods have been used to determine atmospheric DMS levels in field campaigns. Most published methods involve the time-consuming process of trapping atmospheric DMS either in a Pyrex glass tube filled with gold wire or in a canister, and then measuring eluted DMS in a laboratory (Leck and Persson, 1996; Persson and Leck, 1994; Preunkert et al., 2007). In situ measurements have also been performed by concentrating atmospheric DMS in a cryogenic trap from which the DMS was eluted and then analyzed (e.g., Bates et al., 1990; Cooper and Saltzman, 1991; De Bruyn et al., 2002; Kim et al., 2000, 2004; Swan et al., 2015).

The in-situ measurement systems include a component for DMS trapping and elution and a gas chromatograph (GC) equipped with a pulsed flame photometric detector (PFPD) enabling DMS quantification. However, not all components were completely automated and integrated and, as a result, considerable manual input is required to operate the systems over extended periods (months to years). Moreover, to ensure measurement accuracy, some of the in situ analytical systems require regular calibration of the GC-PFPD against known moles of DMS released by a permeation tube containing pure liquid DMS. However, the use of this type of DMS standard over extended periods may result in significant uncertainty in DMS measurements because the amount of DMS released from the permeation tube may change over time (Kim et al., 2016). Therefore, another DMS standard should be used in parallel to evaluate the accuracy of the DMS permeation tube. This practice is particularly useful for long-term measurement of atmospheric DMS in remote locations.

A promising alternative analytical system is based on mass spectrometry (e.g., chemical ionization mass spectrometer) (Mungall et al., 2015). This newly introduced system is based on straightforward measurement principles and can provide highly time-resolved data. However, this system is expensive and its long-term durability has yet to be tested in the field.

We described here the key components of a fully integrated, automated analytical system for the continuous measurement of atmospheric DMS mixing ratios over extended periods (>a year). Measurements to assess its performance over 3 full growing seasons of phytoplankton demonstrated the consistency of the analytical system. Atmospheric DMS concentrations measured using the analysis system at the Zeppelin observatory (Svalbard, Norway) are also presented to highlight the utility of the proposed measurement protocol.

2. Materials and procedures

2.1. Components of the DMS analytical system

The analytical system for measuring atmospheric DMS mixing ratio comprised: (i) a thermostat-controlled inlet for maintaining the temperature of incoming ambient air approximately constant (i.e. to prevent the sudden influx of cold sample); (ii) an integrated unit for DMS trapping and desorption; (iii) a PFPD (Model 5830, OI Analytical, USA) housed in a GC (Agilent 6890N, Agilent Technologies, USA); and (iv) a calibration unit for the detector (Fig. 1). To detect low levels of atmospheric DMS (<1.5 pptv), a trap half-filled with Tenax TA 60–80 mesh (120 mg; Chrompack Inc., USA) and a graphitized carbon trap (U-T14H2S, MARKES International, UK) were used for the 2010 and 2014–2015 field campaigns, respectively. The DMS trapping efficiency of the Tenax TA trap has been reported to be stable over a temperature range of −10 °C to 50 °C (Zemmelink et al., 2002). A DB-1 GC column (30 m long, 0.32 mm diameter, 5.0 μm pore size, J&W Scientific, USA) was used to separate the DMS peak from other chemical signals.

The PFPDs have been shown to be far superior to the flame photometric detectors (FPDs) in detection sensitivity (two orders of magnitude more sensitive) and consumes less H_2 and air (a factor of 20 less) (Cheskis et al., 1993). Therefore, PFPDs are commonly used for measuring reduced sulfur compounds, and have been shown to perform reliably (Steudler and Kijowski, 1984). The response of PFPDs is sensitive to the tuning conditions including the ratio of gases (H_2, air and He), the photomultiplier tube (PMT) voltage, and other factors. In particular, the PMT voltage needs to be adjusted to a specific level for optimal sensitivity for the target concentrations of the sulfur compounds, and the voltage chosen influences the linearity of the detection response (Kim, 2005). As a result, the tuning conditions are important in achieving optimal detector response for the target DMS concentrations. Detailed information about the components of the analytical system and its operating parameters are given in Table 1.

The proposed DMS system was remotely controlled throughout the study period. All required maintenances including the replacement of gases (H_2, air and He) and an oxidant and moisture scrubber were performed by local engineers at the Zeppelin observatory.

2.2. Sequence of DMS analysis

Analysis of atmospheric DMS mixing ratios using the analysis system described above was executed in a sequence involving pre-purging of the DMS trap, DMS trapping and subsequent elution, and DMS analysis. More detailed information on each measurement event (valve control, trap temperature, and the duration of each event) is given in Table S1. Prior to introducing the ambient air to the trap, the trap was flushed for 5 min using ultra-pure He gas (99.99%) to remove any DMS residue from the previous air sample analyzed. To achieve this, valve 2 (V2 in Fig. 1; Valco Instrument Co. Inc., USA) was set to the “on” position.

In operation, the stream of air flows through a thermostat-controlled inlet and a scrubber packed with KI and K_2CO_3 to ensure that oxidants and moisture are removed before the air sample reaches the DMS trap. The air sample was then drawn through a PTFE line at a rate of 100 mL min^{-1} for 10–90 min using a diaphragm vacuum pump (PM24463-86, KNF Neuberger, Germany). The duration of this process was determined by the atmospheric DMS mixing ratio and a mass flow controller (MODEL 3660, KOFLOC, Japan) that controlled the flow rate when V2 was set to the “off” position. The optimal volumes of air needed for an effective detection are shown in Table S2. When a sufficient amount of DMS for analysis has been trapped, the trap is heated to ~220 °C using a custom-made thermoelectric unit (Park and Lee, 2008), and the DMS is eluted from the trap. The thermoelectric unit increases the trap temperature from 20 °C to 220 °C within 1.5 min. In parallel, V2 is set to the “on” position, and He gas carries the eluted DMS into the GC column. The procedure for DMS elution and subsequent injection into the GC column takes ~1.5 min. For separation of the DMS, the gases in the trap are transferred to the capillary column in the GC oven at a constant temperature of ~50 °C, over a period of 3 min. The GC oven temperature is increased to ~240 °C to elute the DMS from the column, and ultra-pure He gas passes through the column carries the eluted DMS to the PFPD. A pressure controller built in the GC regulates the flow rate of the He stream containing

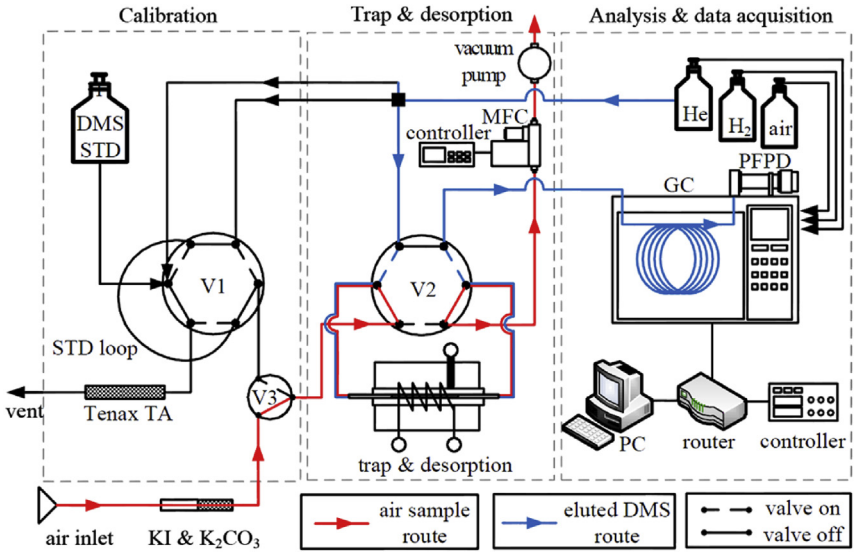

Fig. 1. Schematic representation of the atmospheric DMS measurement system. The system consists of a component for detector calibration, a device for trapping and elution of DMS, and a GC-PFPD for DMS analysis. The red and blue solid lines depict the passages of the air sample and eluted DMS, respectively.

Table 1
Description of analytical system and operating parameters.

Trap	Trap material[a]: (i) Tenax TA 60–80 mesh (ii) Pre-packed column with adsorbent material based on graphitized carbon Trapping temperature: 20 °C Eluting temperature: 220 °C
Column	DB-1, 30 m × 0.32 mm, 5.0 μm, J&W Scientific Temperature: 50 °C–120 °C at 10 °C min^{-1}, 120 °C–240 °C at 50 °C min^{-1} Inlet pressure: 10 psi Carrier gas: He
Detector	Pulsed flame photometric detector (PFPD) Temperature: 250 °C, constant H_2: 9.5 psi, Air: 10.5 psi, He: 10 psi
Calibration	(i) Standard gas: 0.6 to 6.2 ppbv[b], 860, 2850 ppbv (ii) Permeation tube: KIN-TEK, Standard Rate Disposable Permeation Tubes (SRT type), DMS Emission Rate 43 ng min^{-1} at 30 °C

[a] Trap used Tenax TA was custom-made and pre-packed column was a commercial product (U-T14H2S, MARKES International, UK).
[b] DMS working standards were prepared using the dilution method (mixing primary standard of 860 ppbv with ultra-pure N_2).

the eluted DMS.

The DMS peak typically appears between 6.0 and 6.3 min following injection of the eluted DMS into the column. A complete analytical cycle for each air sample usually takes <2 h. Following completion of each analytical cycle, the column in the GC is switched to the flush mode (V2 is set to "off"). The detection limit for the system was found to be 0.02 ng of S, which corresponds to a DMS mixing ratio of approximately 1.5 pptv (when sampled air volume is ~6 L).

2.3. Calculation of atmospheric DMS mixing ratios

Atmospheric DMS mixing ratio (pptv, parts per trillion by volume) is determined using the following equation,

$$\text{DMS (pptv)} = \frac{\sqrt{Peak\ area} - b}{a} \times \frac{R \cdot T}{M_{DMS}} \times \frac{1}{V_{sample}} \times 1000$$

where *Peak area* is the area under the signal of the PFPD response to sulfur. *a* and *b* are the slope and intercept of the calibration curve, respectively; R is the ideal gas constant; T is the sample air temperature; M_{DMS} is the molar mass of DMS; and V_{sample} is the volume of air sampled (1–9 L). Note that $\sqrt{Peak\ area}$ measured by PFPDs is linearly related to sulfur mass analyzed (Cheskis et al., 1993).

2.4. Data acquisition system

All analytical processes, including valve control and the thermoelectric module controlling the DMS trap temperature, are controlled using custom-built software based on Visual Basic 6.0/C 6.0. This software provides a virtual interface, and comprises electronic buttons, switches, and a data display for operating the instrumentation that drives the automated DMS analysis system (Fig. S1). During the field campaigns, the system was connected to the Internet, which enabled the analytical sequences to be remotely controlled.

3. Assessments and discussion

3.1. Preparation of DMS working standards and their accuracy

During the field campaigns, the DMS working standards were prepared by mixing exact amounts of N_2 and a primary standard having a certified value of 552 or 860 ppbv (2.6% uncertainty). In

this gas mixing process, two gases (N_2 and a primary standard) were concurrently introduced at rates of 200–1000 mL min^{-1} and 1–2 mL min^{-1}, respectively, into a 500 mL-PTFE bottle in which a magnetic stirrer continuously mixed the incoming gases. This mixing method ensured the production of homogeneous working standards in terms of the DMS mixing ratios. Our test experiments showed that the DMS mixing ratios in the gas mixture in the PTFE bottle reached a constant value within 60 min following the introduction of the gases in the bottle (Fig. S2). This mixing (or dilution) method accurately produced a set of DMS working standards having a concentration range of 0.6–6.2 ppbv. This range is adequate for measuring the atmospheric DMS mixing ratios that occur over the Arctic Ocean during the phytoplankton bloom period.

The accuracy of the prepared working standards was checked against the certified value of the primary standard (860 ppbv DMS). We found good agreement between the primary and working standards within a mixing ratio range of 0.5–7.0 pmol of DMS (Fig. 2a).

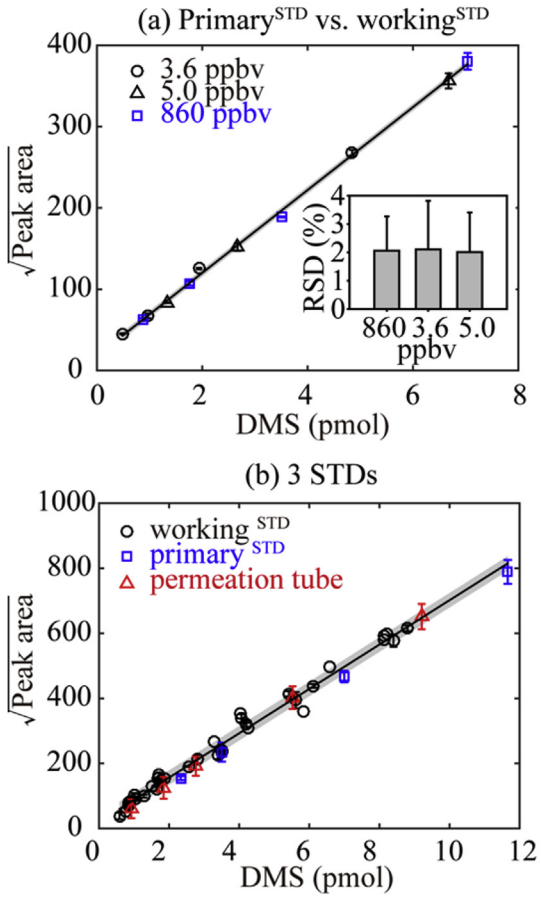

Fig. 2. (a) Relationship of the working standard (STD) measurements (DMS = 3.6 and 5.0 ppbv) to the primary standard (DMS = 860 ppbv). The inset shows the relative standard deviation (the standard deviation divided by the mean) for all standard measurements. The shaded area indicates one standard deviation ($1\sigma = \pm 4.3$) from the best fit. (b) The GC-PFPD calibration results for three types of DMS standard over 3 years during the field campaigns. The calibrations based on working standards, primary standards, and the permeation tube are shown as black circles, blue squares, and red triangles, respectively. The shaded area indicates 1σ (± 22.1) from the best fit. In (a) and (b) the black solid lines indicate the best linear fits for all data. (For interpretation of the references to color in this figure legend, the reader is referred to the web version of this article.)

3.2. Calibration of the GC-PFPD as a DMS detector

During the field campaigns, the response of the GC-PFPD detector was calibrated against at least one of three types of DMS standards: (1) a set of working standards; (2) two primary standards having certified mole factions of 860 and 2850 ppbv; and (3) known moles of DMS released by a permeation tube filled with >99.9% liquid DMS (Sigma-Aldrich, USA).

As a primary method for calibration in 2010, DMS working standards were regularly used to check the stability of the response of the GC-PFPD, so as to minimize the consumption of DMS primary standards. For calibration, working standards were prepared immediately prior to each individual calibration, and various accurately measured volumes of the working standards (3–52 mL) were injected into the detector using a mass flow controller (F-201C-FAC-11-V, Bronkhorst, UK). The amount of DMS in the working standards used for detector calibration ranged from 0.6 to 8.8 pmol.

In 2014, we used two high-pressure DMS standards, which were prepared by Yara Praxair (Norway) in 20-L aluminum cylinders using He as the balance gas. Three volume-calibrated loops (10 μL, 25 μL, 100 μL; Valco instrument Co. Inc., USA) were used to introduce precise amounts of the primary standards to the DMS trap. This method was used to generate DMS standard ranging from 2.3 to 14.1 pmol of DMS for the calibration.

When the two primary standards ran out in 2015, as an alternative we used a DMS permeation tube, through which DMS is released at a constant rate (43 ng min^{-1}). KIN-TEK laboratories (USA) certified the rate of release of DMS from the permeation tube. Varying amounts of He gas flowing into the permeation tube changed the DMS mixing ratio released from the tube. In our analytical setting, the permeation tube was positioned inside a PFA tube, through which the He flowed at a rate of 69 mL min^{-1}; the resulting DMS mixing ratio was 225 ppbv. The DMS released from the permeation tube filled a 100-μL sample loop installed in the six-port valve (V1), and was then injected into the detector for calibration (Fig. 1). The calibration results based on use of the permeation tube were consistent with those based on use of the primary and working gas standards (Fig. 2b). Such good consistent calibration results indicate that small temperature fluctuation (±1.3 °C) in the PFA during the field operation did not seriously bias our results (<6.3%). This method covered the DMS standard ranging from 0.9 to 9.2 pmol of DMS.

The detector response needs to be calibrated in a DMS concentration range that is comparable to that in air samples being analyzed. In our detector calibration measurements within the range of DMS_{pmol} = 0.6–11.7, the detector response ($\sqrt{\text{Peak area}}$) increased linearly with increasing amounts of DMS injected. The DMS mixing ratios in air samples that fell out of this calibration range were calculated by extrapolation from the calibration curves. In particular, when the calibration curves were extrapolated to the peak area for zero, when no DMS was added, the error in calculation of the DMS mixing ratio for samples having small peak areas (<5000) was <0.9 pptv (Table S3).

For all the calibration curves obtained over 3 full annual growth cycles of phytoplankton, the detector response showed good linearity (Fig. 2b). All daily calibration curves were internally consistent within a 6-month period, except for May 2014, during which a change in the detector response was discernable, and probably resulted from changes in the lower PMT voltage in the detector and changes in the ratio of combustion gases (H_2, air and He). The calibration curve in May 2014 still showed good linearity (R^2 = 0.99), and was suitable for calculation of atmospheric DMS mixing ratios (Fig. S3).

3.3. DMS trapping efficiency

The trapping efficiency for DMS was measured by comparing the response of the detector to identical amounts of the standard gas injected (i) directly into the GC-PFPD, or (ii) added to the DMS trap, eluted, and then injected from the trap into the detector. In our test comparison we used a 100 μL volume of the 860 ppbv DMS standard. The value for direct injection did not differ statistically from the value obtained using the DMS trap. The results indicated that the trapping efficiency was 98.1% (Table S4).

3.4. Long-term consistency of the DMS analytical system

The overall performance of the key components of the analytical system was evaluated using two independent methods. In 2010 (between March and December) we occasionally checked the performance of the system by measuring DMS of a working standard having a mixing ratio of 4.1 ppbv. The results did not change systematically over time and were consistent within 4.3% (Fig. 3a), indicating that the detector did not drift during the entire period of operation. This single-point checking of stability was not undertaken during the 2014 and 2015 field campaigns, when instead we occasionally performed multi-point calibrations. The calibration curves resulting from analysis of multiple standards did not show any systematic trends over time; the slope of the calibration curves (a good indicator of detector sensitivity) changed from 63.6 to 75.7 ($1\sigma = \pm 3.5$). This also indicated that the performance of the analytical system remained consistent during this 2-year period (Fig. 3b).

The uncertainty in atmospheric DMS measurements performed using the proposed analytical system was approximately 5% (Table 2); this value was obtained using the uncertainties associated with all of the individual procedures involved in atmospheric DMS measurement, according to the guide of Ellison and Williams (2012).

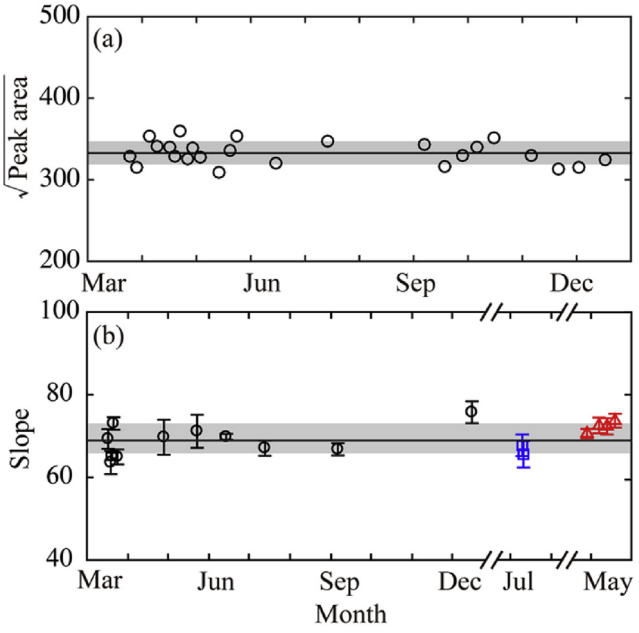

Fig. 3. (a) Detector response for all measurements of a single DMS working standard (4.1 ppbv, 24 mL) (mean response = 333), made in 2010. The shaded area indicates one standard deviation from the mean ($1\sigma = \pm 14.3$), and the analytical repeatability of these measurements was 4.3%. (b) Slopes for all calibration curves obtained over 3 full annual growth cycles of phytoplankton (the mean slope = 69.3). Different colored symbols indicate different calibration methods indicated in the caption to Fig. 2. The shaded area in (b) indicates one standard deviation (±3.5) from the mean. The error bars indicate the standard errors of each slope. (For interpretation of the references to color in this figure legend, the reader is referred to the web version of this article.)

Table 2
Estimations of relative standard uncertainty (referred to as "uncertainty" hereinafter) for 3 types of standard (STD) and atmospheric DMS measurements.

Types of STD	Certified values	Volume injected		STD injected[f]	Air DMS[g]
		Loop[d]	MFC[e]		
Primary	2.6%[a]	0.5%	–	2.6%	5.0%
Working	2.6%[b]	–	0.3%	2.6%	5.1%
Permeation	2.9%[c]	0.5%	–	3.0%	5.3%

[a] Calculated by dividing the accuracy of 5% (with a 95% confidence level; the accuracy and its confidence level were provided by the manufacturer) by 1.96 (Ellison and Williams, 2012).
[b] Calculated using the square root of the sum of the squares of the uncertainties in the certified value of the primary STD and the amounts of the primary STD and N_2 gas used for the preparation of the working STD using a mass flow controller (MFC; F-201C-FAC-11-V, Bronkhorst, UK).
[c] Calculated using the square root of the sum of the squares of the uncertainty in the accuracy of the rate of DMS released from a permeation using a MFC (MODEL 3660, KOFLOC, Japan).
[d] Uncertainty in the volume of STD injected into the detector via a standard loop was directly measured using the water-based gravimetric method (i.e., measure the mass difference between a loop filled with water and the loop when empty, and then divide the mass difference obtained by the water density at the time of measurement) (Wilke et al., 1993).
[e] Uncertainty in the volume of STD injected into the detector using a MFC was calculated by dividing the accuracy of 0.5% (provided by the manufacturer without the confidence level information) by $\sqrt{3}$, given that measurements of sample volumes using a MFC are rectangularly distributed.
[f] Calculated using the square root of the sum of the squares of the uncertainties in the preparation of the STD (2nd column) and the volume of STD injected (either 3rd or 4th columns).
[g] Calculated using the square root of the sum of the squares of the uncertainties in the amount of DMS STD injected into the detector, the volume of air sample injected using a MFC (MODEL 3660, KOFLOC, Japan), and the PFPD response (4.3%, the repeatability of the detector response; see results in Fig. 3a).

3.5. Atmospheric DMS mixing ratios over the Arctic Ocean

The system for atmospheric DMS analysis was installed at the Zeppelin observatory in March 2010, and thereafter was used for measurement of atmospheric DMS mixing ratios in the Atlantic sector of the Arctic Ocean over 3 full annual growth cycles of phytoplankton.

The measured mixing ratios differed strikingly among seasons and years (Fig. 4a). The measured mixing ratios increased by 100–450 pptv in May and June each of the three years, and showed considerable short-term (<a few days) and long-term (one week to one year) variability; however, the mixing ratios declined rapidly by an order of magnitude thereafter, and remained at that level until the end of the growing season (the end of July). Throughout winter (September to April), which was characterized by an analytical detection limit of 1.5 pptv DMS, almost no atmospheric DMS mixing ratio was detectable (not shown in Fig. 4a). In the dataset for each of the 3 years the atmospheric DMS mixing ratios varied on a timescales of < one week, which is best explained by the changes in the meteorological parameters (air mass trajectory, altitude and speed) (Park et al., 2013).

To assess whether there was a direct relationship between the air mass trajectory and short-term (<a few days) variability in the DMS mixing ratios, we examined the selected 2-day air mass back-trajectories prior to them reaching the Zeppelin observatory.

The mean chl-*a* concentration in May 2015 and the 2-day back-trajectories are shown in Fig. 4b and c. The black line in Fig. 4b

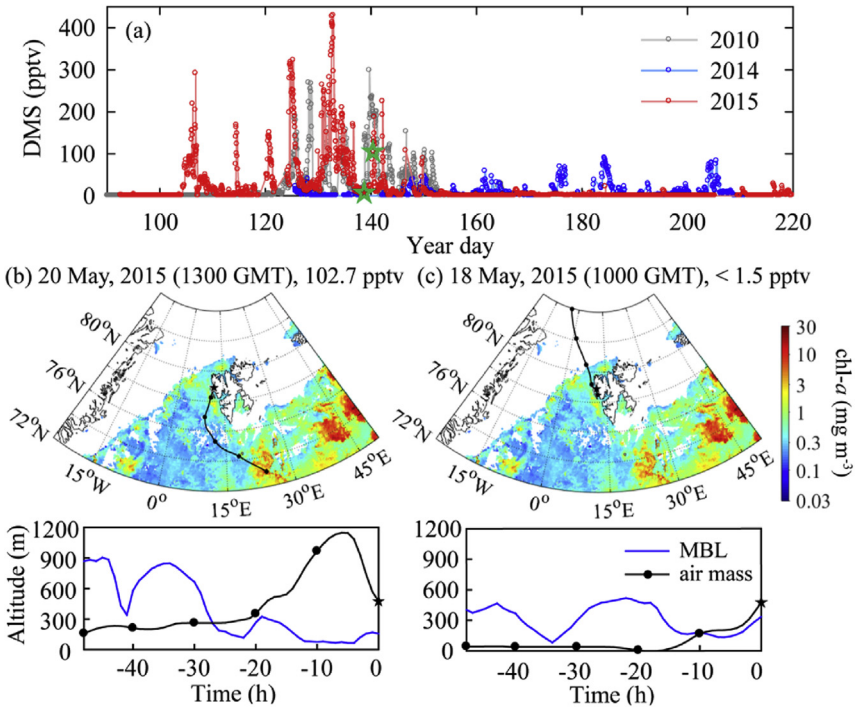

Fig. 4. (a) Mixing ratios of atmospheric DMS at Zeppelin observatory from March to July in 2010, 2014, and 2015. (b, c) Monthly mean chl-*a* concentration during the month of May in 2015 (at a 4 km resolution, obtained from the Moderate-Resolution Imaging Spectroradiometer (MODIS) on the satellite Aqua), overlaid with the 2-day air mass back-trajectories corresponding to the two green stars shown in (a). The rectangular panels below the chl-*a* maps show the evolution of air mass altitudes and the marine boundary layers (MBL) during the 2-day air mass back-trajectories. The black circles in (b), (c), and the panels correspond to positions and altitudes of air masses at 10, 20, 30, 40, and 48 h prior to arrival of the air masses at the Zeppelin observatory and the black stars in (b), (c), and the panels indicate the Zeppelin site (78.5°N, 11.8°E, 474 m above sea level). Note that the Hybrid Single-Particle Lagrangian Integrated Trajectory model was used to calculate air mass back-trajectories and marine boundary layers (Draxler and Hess, 1998).

corresponded to the air mass back-trajectory estimated for 20 May 2015, which had a high DMS mixing ratio (102.7 pptv; Fig. 4a); this air mass passed over a region having high chl-*a* and DMS concentrations. In contrast, the black line in Fig. 4c corresponded to the back-trajectory estimated for 18 May 2015, which had a DMS mixing ratio below the detection limit (<1.5 pptv; Fig. 4a); this air mass passed over a region having low chl-*a* and DMS concentrations. These contrasting back-trajectory examples showed that the air masses reflected the source strength of that ocean surface (below the marine boundary layer) of the region over which they passed (Fig. 4b and c). The results support the hypothesis that the chl-*a* concentration, species composition, and other properties vary among ocean domains, and that this contributes to variations in atmospheric DMS.

4. Conclusion

The atmospheric DMS measurement system described here proved to be robust, efficient, and enabled continuous near real-time quantification of DMS mixing ratios in the remote atmosphere. The advantages of the system include the ability to accurately analyze multiple samples (1–2 h per sample) without interruption, its low detection limit (1.5 pptv DMS in 6 L of sample air), automated data collection, and remote control of the system. The system can be used to measure both short-term and long-term trends in atmospheric DMS. It requires minimal weekly maintenance, and can provide continuous reliable atmospheric DMS mixing ratio data. Data on atmospheric DMS mixing ratios in combination with other datasets (e.g. satellite chl-*a*, aerosols, and meteorological data) will provide critical insights into the major drivers of emission of DMS into the atmosphere. In particular, the system will be useful for detecting changes in DMS production associated with Arctic Ocean acidification and sea ice melting.

Acknowledgements

We thank the Sverdrup Research Station staffs of the Norwegian Polar Institute for assisting us to maintain the atmospheric DMS analysis system at Zeppelin station. This research was primarily supported by Mid-career Researcher Program (No. 2015R1A2A1A05001847) funded by the National Research Foundation (NRF) of Ministry of Science, ICT and Future Planning. Partial supports were provided by Global Research Project (2013K1A1A2A02078278) funded by NRF; "Management of Marine Organisms causing Ecological Disturbance and Harmful Effects" by the Ministry of Oceans and Fisheries; "The GAIA Project (2014000540010)" by Korea Ministry of Environment, and by MSIP (NRF-C1ABA001-2011-0021063); and a grant from the National Fisheries Research and Development Institute (R2016051).

Appendix A. Supplementary data

Supplementary data related to this article can be found at http://dx.doi.org/10.1016/j.atmosenv.2016.03.041.

References

Andreae, M.O., Crutzen, P.J., 1997. Atmospheric aerosols: biogeochemical sources and role in atmospheric chemistry. Science 276, 1052–1058.
Andreae, M.O., Rosenfeld, D., 2008. Aerosol-cloud-precipitation interactions. Part 1. The nature and sources of cloud-active aerosols. Earth Sci. Rev. 89, 13–41.
Bates, T.S., Charlson, R.J., Gammon, R.H., 1987. Evidence for the climatic role of marine biogenic sulphur. Nature 329, 319–321.
Bates, T.S., Johnson, J.E., Quinn, P.K., Goldan, P.D., Kuster, W.C., Covert, D.C.,

Hahn, C.J., 1990. The biogeochemical isulfur cycle in the marine boundary layer over the northeast Pacific Ocean. J. Atmos. Chem. 10 (1), 59–81.
Charlson, R.J., Lovelock, J.E., Andreae, M.O., Warren, S.G., 1987. Oceanic phytoplankton, atmospheric sulphur, cloud albedo and climate. Nature 326, 655–661.
Cheskis, S., Atar, E., Amirav, A., 1993. Pulsed-flame photometer: a novel gas chromatography detector. Anal. Chem. 65, 539–555.
Cooper, D.J., Saltzman, E.S., 1991. Measurements of atmospheric dimethyl sulfide and and carbon disulfide in the western Atlantic boundary layer. J. Atmos. Chem. 12 (2), 153–168.
De Bruyn, W.J., Harvey, M., Cainey, J.M., Saltzman, E.S., 2002. DMS and SO_2 at baring head, New Zealand: implications for the yield of SO2 from DMS. J. Atmos. Chem. 41 (2), 189–209.
Draxler, R.R., Hess, G.D., 1998. An overview of the HYSPLIT_4 modeling system for trajectories, dispersion and deposition. Aust. Meteorol. Mag. 47, 295–308.
Ellison, S.L., Williams, A., 2012. Quantifying Uncertainty in Analytical Measurement, third ed. EURACHEM/CITAC.
Kim, K.-H., Lee, G., Kim, Y.P., 2000. Dimethylsulfide and its oxidation products in coastal atmospheres of Cheju Island. Environ. Pollut. 110 (1), 147–155.
Kim, K.-H., Swan, H., Shon, Z.H., Lee, G., Kim, J., Kang, C.H., 2004. Monitoring of reduced sulfur compounds in the atmosphere of Gosan, Jeju Island during the spring of 2001. Chemosphere 54 (4), 515–526.
Kim, K.-H., 2005. Performance characterization of the GC/PFPD for H_2S, CH_3SH, DMS, and DMDS in air. Atmos. Environ. 39, 2235–2242.
Kim, M.E., Kim, Y.D., Kang, J.H., Heo, G.S., Lee, D.S., Lee, S., 2016. Development of traceable precision dynamic dilution method to generate dimethyl sulphide gas mixtures at sub-nanomole per mole levels for ambient measurement. Talanta 150, 516–524.
Leck, C., Persson, C., 1996. Seasonal and short-term variability in dimethyl sulfide, sulfur dioxide and biogenic sulfur and sea salt aerosol particles in the arctic marine boundary layer during summer and autumn. Tellus 48B, 272–299.
Mungall, E.L., Croft, B., Lizotte, M., Thomas, J.L., Murphy, J.G., Levasseur, M., Martin, R.V., Wentzell, J.J.B., Liggio, J., Abbatt, J.P.D., 2015. Summertime sources of dimethyl sulfide in the Canadian Arctic Archipelago and Baffin Bay. Atmos. Chem. Phys. Discuss. 15 (24), 35547–35589.
Park, K.-T., Lee, K., 2008. High-frequency, accurate measurement of dimethylsulfide in surface marine environments using a microporous membrane contactor. Limnol. Oceanogr. Methods 6, 548–557.
Park, K.-T., Lee, K., Yoon, Y.-J., Lee, H.-W., Kim, H.-C., Lee, B.-Y., Hermansen, O., Kim, T.-W., Holmen, K., 2013. Linking atmospheric dimethyl sulfide and the Arctic Ocean spring bloom. Geophys. Res. Lett. 40, 155–160.
Persson, C., Leck, C., 1994. Determination of reduced sulfur compounds in the atmosphere using a cotton scrubber for oxidant removal and GC with flame photometric detection. Anal. Chem. 66, 983–987.
Preunkert, S., Legrand, M., Jourdain, B., Moulin, C., Belviso, S., Kasamatsu, N., Fukuchi, M., Hirawake, T., 2007. Interannual variability of dimethylsulfide in air and seawater and its atmospheric oxidation by-products (methanesulfonate and sulfate) at Dumont d'Urville, coastal Antarctica (1999–2003). J. Geophys. Res. 112. D06306.
Shaw, G., 1983. Bio-controlled thermostasis involving the sulfur cycle. Clim. Change 5, 297–303.
Simó, R., 2001. Production of atmospheric sulfur by oceanic plankton: biogeochemical, ecological and evolutionary links. Trends Ecol. Evol. 16, 287–294.
Stefels, J., Steinke, M., Turner, S., Malin, G., Belviso, S., 2007. Environmental constraints on the production and removal of the climatically active gas dimethylsuphide (DMS) and implications for ecosystem modelling. Biogeochemistry 83, 245–275.
Steudler, P.A., Kijowski, W., 1984. Determination of reduced sulfur gases in air by solid adsorbent preconcentration and gas chromatography. Anal. Chem. 56, 1432–1436.
Swan, H.B., Ivey, J.P., Jones, G.B., Eyre, B.D., 2015. The validation and measurement uncertainty of an automated gas chromatograph for marine studies of atmospheric dimethylsulfide. Anal. Methods 7 (9), 3893–3902.
Wilke, R.J., Wallace, D.W.R., Johnson, K.M., 1993. Water-based, gravimetric method for the determination of gas sample loop volume. Anal. Chem. 65 (17), 2403–2406.
Zemmelink, H.J., Gieskes, W.W.C., Holland, P.M., Dacey, J.W.H., 2002. Preservation of atmospheric dimethyl sulphide samples on Tenax in sea-to-air flux measurements. Atmos. Environ. 36, 911–916.